



ELSEVIER

Contents lists available at ScienceDirect

## Mechanics of Materials

journal homepage: [www.elsevier.com/locate/mechmat](http://www.elsevier.com/locate/mechmat)

## Shear banding in sub-microcrystalline nickel at 4 K

S.R. Dey<sup>a,b</sup>, L. Hollang<sup>b</sup>, B. Beausir<sup>b,c</sup>, E. Hieckmann<sup>d</sup>, W. Skrotzki<sup>b,\*</sup><sup>a</sup> Department of Materials Science and Engineering, Indian Institute of Technology Hyderabad, Yeddumailaram 502205, India<sup>b</sup> Institut für Strukturphysik, Technische Universität Dresden, 01062 Dresden, Germany<sup>c</sup> Laboratoire d'Etude des Microstructures et de Mécanique des Matériaux (LEM3), Université Paul-Verlaine de Metz, 57012 Metz, France<sup>d</sup> Institut für Angewandte Physik, Technische Universität Dresden, 01062 Dresden, Germany

## ARTICLE INFO

## Article history:

Received 23 July 2012

Received in revised form 24 January 2013

Available online 20 July 2013

## Keywords:

Nickel

Sub-microcrystalline

Shear banding

Texture

## ABSTRACT

A flat specimen of sub-microcrystalline nickel was tensile tested at 4 K until fracture occurred and subsequently investigated by electron backscatter diffraction in a high resolution scanning electron microscope in order to deduce the local texture in the near crack area. Thus, two sets of intersecting fine slip markings observed on the surface (under  $\pm 55^\circ$  with respect to the tensile axis) could be explained as a result of localized simple shear in the bulk material underneath the slip markings. The overall amount of shear in the region near the crack was estimated to be 1.25 based on texture simulations using the viscoplastic self-consistent polycrystal model.

© 2013 Published by Elsevier Ltd.

## 1. Introduction

Grain size and temperature affect the strength of materials. Generally, diminishing the grain size and lowering the temperature increase their strength. However, these beneficial effects are limited since at a certain stress level the deformation mode changes from homogeneous plastic deformation towards localized plastic flow. This finding is not new, but was first published in 1860 (Lüders, 1860) and is nowadays also found in sub-microcrystalline and nanocrystalline metals tested in tension (e.g. Yu et al., 2005; Park et al., 2010) as well as in compression (e.g. Wei et al. 2002). Despite the overwhelming technological relevance very little is still known regarding the mechanisms responsible for the onset and subsequent persistence of localized shear in sub-microcrystalline and nanocrystalline metals.

Since the time of Lüders (1860) surface slip markings appearing during uniaxial deformation are known to be a common feature of metal single and polycrystals. Pronounced surface slip markings often indicate the onset of

localized slip as it was shown for single crystalline metals (e.g. Niewczas et al., 2001a) as well as sub-microcrystalline and nanocrystalline metals (Vinogradov et al., 2001; Wei et al., 2002). The paper aims to correlate such surface slip markings (traces of shear bands) observed after deformation at very low temperatures with microstructural features in the bulk in the model system “pure sub-microcrystalline nickel”. The paper continues the texture investigations based on conical dark field measurements on a cylindrical specimen deformed in tension at 4 K (Dey et al., 2010a; unfortunately, the abscissa of Fig. 2 in this paper is wrong and has to be divided by 3). The observation of Dey et al., 2010a was that the initially homogeneous deformation suddenly changed towards repeated “catastrophic” shear events at about 2400 MPa. After a first stress drop of 16.9% the deformation continued until a second stress drop of the same order appeared. Also the second event was not fatal for the specimen. Again the deformation continued, but then the specimen failed during a third shear event. The shear events were accompanied by loud acoustic emission. TEM micrographs taken from the catastrophic sheared region showed a substantial elongation of grains between growth direction and tensile axis. The pole figures from the sheared region presented deviations from the initial texture and were found to be

\* Corresponding author. Tel.: +49 351 463 35144; fax: +49 351 463 37048.

E-mail address: [werner.skrotzki@tu-dresden.de](mailto:werner.skrotzki@tu-dresden.de) (W. Skrotzki).

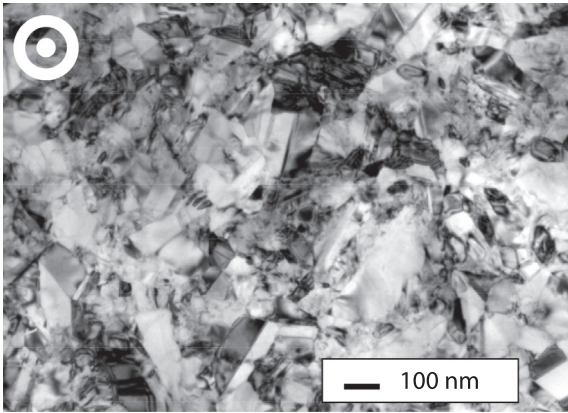


**Fig. 1.** TEM image of the PED plate in the initial state. The growth direction is perpendicular to the image plane.

comparable with the typical shear texture obtained from the operation of fcc  $\{111\}\langle 110 \rangle$  slip systems. The conclusion was that in the localized shear zone the deformation is carried by dislocation slip. It was argued that the trigger mechanism for the onset of strain localization is probably related to twinning.

In this paper the tools are wide-ranging (compared with conical dark field measurements) surface measurements on a flat specimen performed in high resolution in a scanning electron microscope (SEM) and detailed investigations of local texture using electron backscatter diffraction (EBSD). The measured textures are finally connected with advanced texture simulations which yield information on the deformation process the material has experienced. Such conclusions are possible since the type of texture depends on the deformation mode. For example, if dislocation slip is dominating during deformation in

uniaxial tension and compression typical fibre textures develop having axial symmetry, while for rolling and simple shear they have orthorhombic and monoclinic symmetry, respectively (Engler and Randle, 2010). In contrast, if grain boundary sliding is the dominating deformation mechanism, texture formation is suppressed (Ivanisenko et al., 2012).

## 2. Material and experimental methods

The sub-microcrystalline nickel discussed in this paper was already characterized elsewhere (Dey et al., 2010a; Hollang et al., 2010). A brief description of the initial state reads as follows: A rectangular slab ( $70 \times 40 \times 2 \text{ mm}^3$ ) of additive-free sub-microcrystalline nickel was produced using the pulsed electrodeposition technique in a sulfate bath without additives for grain refinement (e.g. saccharin). The initial microstructure of the plate was investigated by X-ray diffraction measurements, electron backscatter diffraction (EBSD) and transmission electron microscopy (TEM: Phillips CM 200). The TEM foil was produced by conventional electrochemical dimpling (Struers Tenupol). A representative TEM image with growth direction (GD) parallel to the image plane is shown in Fig. 1. The evaluation of X-ray line profiles using an altered Williamson–Hall (WH) plot yielded a size of “coherently scattering domains”  $d_{\text{WH}} \approx 35 \text{ nm}$  and a rather high level of the “root mean square stresses”  $\langle \sigma_{\text{rms}}^2 \rangle^{1/2} \approx 200 \text{ MPa}$ . However, the average grain size  $d_{\text{EBSD}} = 140 \text{ nm}$  obtained from large scale EBSD images ( $230 \times 170 \mu\text{m}^2$ ) was found to be 5 times higher than  $d_{\text{WH}}$ . It was either 150 nm or 130 nm if determined from the image taken parallel or perpendicular to GD, respectively. There was a weak  $\langle 110 \rangle$  fibre texture along GD.

The dog-bone shaped flat tensile specimen with 10 mm gauge length (rectangular cross section  $3.80 \times 0.24 \text{ mm}$ , cf.

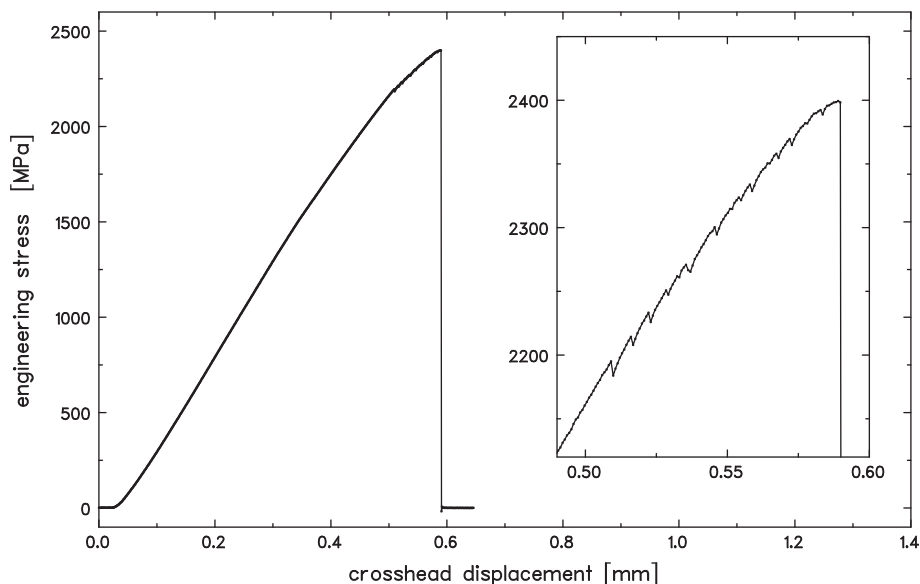


**Fig. 2.** Stress–displacement curve of the sub-microcrystalline Ni specimen tested at 4 K. Inset shows the part above 2100 MPa characterized by sudden small stress drops. At about 2400 MPa sudden fracture terminated the deformation experiment.

Fig. 2) with GD perpendicular to the flat surface was cut by spark erosion, subsequently mechanically ground and finally electropolished. The tensile test was performed at 4 K in an Instron 4502 load frame equipped with an open continuous flow cryostat with liquid He coolant (Brunner and Diehl, 1992) at a constant cross head displacement rate of 0.086 mm/min, thus providing an initial plastic strain rate of about  $10^{-4} \text{ s}^{-1}$ .

The quantitative microstructure and texture analysis is based on EBSD measurements. The investigations were performed in a Zeiss Ultra 55 equipped with a field emission gun. The shear texture measured in the region near the crack was simulated with the viscoplastic self-consistent polycrystalline (VPSC) model (version 7b). For details of the basic principles (e.g. the definition of “shear” used) see Hill (1965), Molinari et al. (1987) and Lebensohn and Tomé (1993). In order to meet the experimental observations (slip markings appear under  $55^\circ$ , see below), two shears in the plane normal to the tensile axis (TA) are superimposed: The first is negative in the  $55^\circ$ -direction with respect to TA while the second is positive in  $125^\circ$ -direction (see Fig. 2c). By considering the same amount of shear  $\gamma$  in the two shear systems, the corresponding velocity gradient  $\underline{\mathbf{L}}$  is given in the basis  $(\mathbf{e}_1, \mathbf{e}_2, \mathbf{e}_3) = (\text{TA}, \text{ND}, \text{GD})$  by:

$$\underline{\mathbf{L}} = \underline{\mathbf{L}}^\lambda + \underline{\mathbf{L}}^{\pi-\lambda} = \dot{\gamma} \sin(2\lambda)(\mathbf{e}_1 \otimes \mathbf{e}_1 - \mathbf{e}_2 \otimes \mathbf{e}_2), \quad (1)$$

with  $\lambda = 55^\circ$ . From Eq. (1) it is clear that the combination of these two shears leads to tension along TA and compression along ND in equal proportion. Only octahedral glide  $\{111\}\langle 110\rangle$  is considered in the simulation and no hardening is imposed on the slip systems. The input texture is composed of 3000 grain orientations obtained from the EBSD measurement. Several values of  $\gamma$  as well as strain-rate sensitivity  $m$  were tested in the simulations.

### 3. Results and discussion

Fig. 2 shows the engineering stress as function of the cross head displacement. The specimen exhibits the strong parabolic hardening behavior typical for sub-microcrystalline and nanocrystalline metals at low temperatures (Hollang et al., 2006). However, at 2200 MPa the smooth steep rise in stress with ongoing displacement is followed by some sort of “jerky flow” characterized by sudden small stress drops as shown detailed in the inset of Fig. 1.

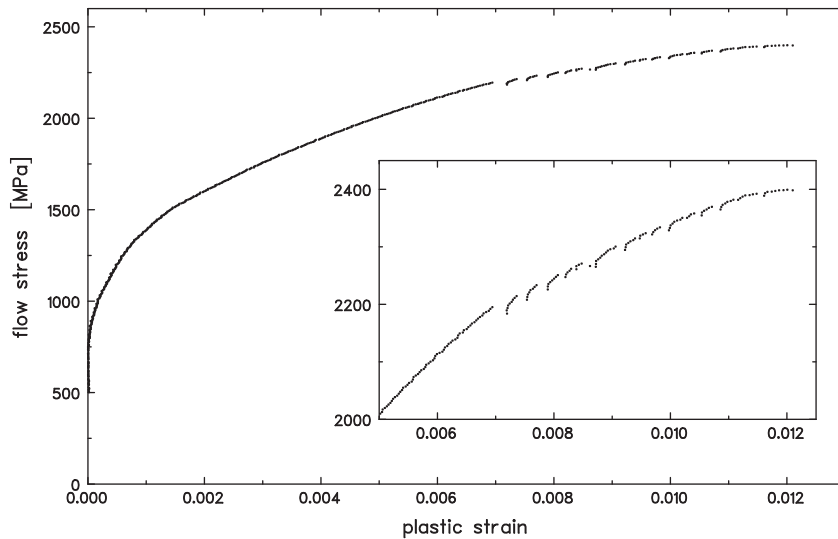
At about 2400 MPa sudden fracture terminated the deformation experiment after only 1.2% plastic strain as the hardening coefficient reaches zero. This can be seen clearly in Fig. 3, which shows the flow stress as a function of plastic strain. The latter could not be measured directly at the specimen, but was calculated from the cross-head displacement for a gauge length of 10 mm (Hollang et al., 2006). The stress drops shown in Fig. 2 are now accompanied by “strain gaps” in Fig. 3. For example, the first three strain gaps visible in Fig. 2 (see inset) are the result of a sudden plastic straining of about 0.02% in each case. Each stress drop is followed by elastic reloading. Afterwards the material deforms plastically for a short while before another stress drop occurs.

Generally, the flat specimen behaves very similar if compared with the cylindrical one discussed by the authors in Ref. Dey et al. (2010a) and mentioned briefly in the introduction above. Particularly, this holds for the ultimate tensile stress, which is about 2400 MPa in both cases. However, the flat specimen behaves differently in two remarkable senses. First of all, after 0.7% plastic strain the appearance of the small stress drops announces some changes in deformation mode. And secondly, after further 0.5% plastic straining in “discontinuous” deformation mode sudden fracture occurred as the strain hardening coefficient reached zero.

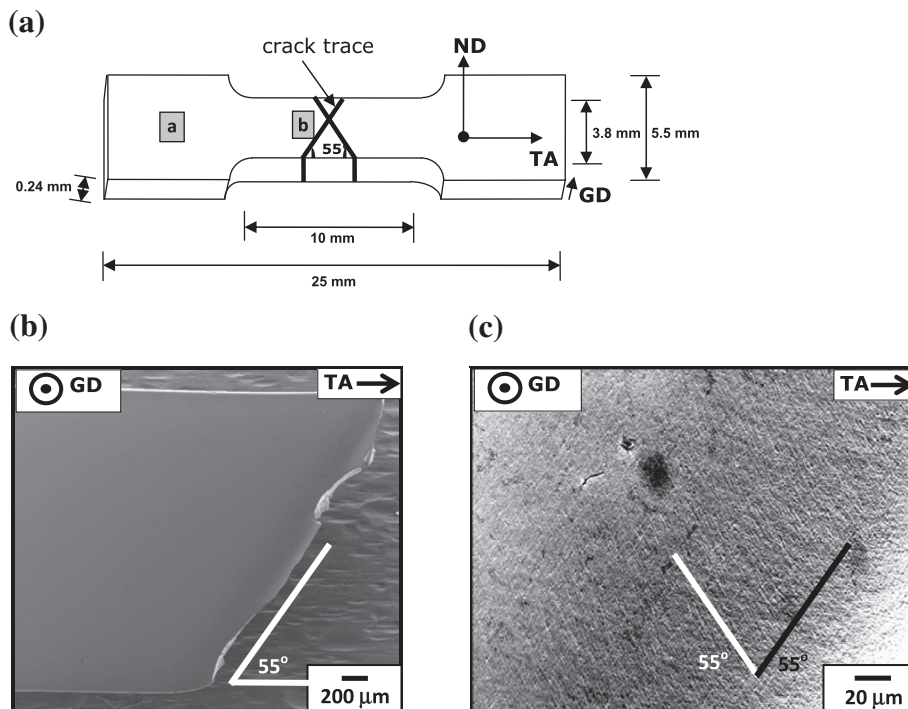
The small stress drops observed are unique in the context of the sub-microcrystalline nickel discussed here, but seem to be very similar to those observed by Niewczas et al. (2001a) and Niewczas et al. (2001b), in copper single crystals tested at 4.2 K. They argue that the onset of twinning acts as trigger for adiabatic deformation if the stress reaches the level necessary to nucleate twins. Despite the differences between single crystalline copper and sub-microcrystalline nickel the present authors argue that twinning may also act as a trigger for the onset of local shear banding in sub-microcrystalline nickel, where the deformation proceeds by conventional dislocation slip (Dey et al., 2010a). The authors argue that the shear band propagation exhausts itself very fast at stresses below 2400 Mpa, while it is accelerated by local “deformation heating” of the specimen (see, e.g. Zaiser and Hähner, 1997) at 2400 MPa, which therefore is a threshold stress. Indeed, Tabachnikova et al., 2010, observed “traces of melting” on the failure surface of 22 nm Ni–20% Fe compression samples deformed at 170 K and 77 K after fatal failure by shear banding under  $45^\circ$ . Due to the high temperature and experimental rate sensitivity of the material this “deformation heating” really has a “catastrophic” effect.

This explanation differs somewhat from that of Rösner et al. (2009) found for the failure of nanocrystalline Pd and Pd<sub>90</sub>Au<sub>10</sub> during in situ tensile tests at ambient temperature. They found intergranular fracture to be the main response of the material and argued that an early onset of the limit to plastic flow is responsible because dislocation-based deformation processes are not able to operate sufficiently within the small grains to relax stress concentrations prior to fracture. In some cases deformation twins were formed in Pd and Pd<sub>90</sub>Au<sub>10</sub> due to the stress field of the advancing crack tip providing favorable intragranular propagation paths for the crack tip. A rather obvious consequence of this cracking mechanism found by Rösner et al. (2009) is the lack of any texture evolution near the crack surface. However, pronounced slip markings as well as a distinct shear texture in the region next to the crack are key features of the sub-microcrystalline nickel after deformation at 4 K. This will be discussed next.

The dimensions, coordinate system, surface shear and crack traces of the deformed flat tensile specimen are schematically sketched in Fig. 4a. The surprisingly straight crack line is inclined under  $55^\circ$  with respect to TA, Fig. 4b. Surprisingly, this corresponds to the inclination angles frequently observed in metallic glasses tested in tension at room temperature (e.g. Mukai et al., 2002;



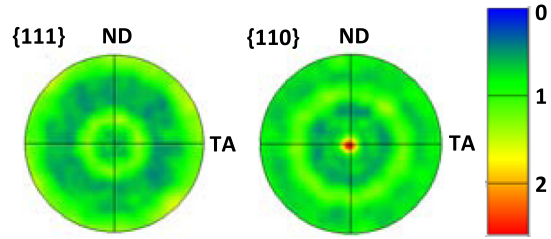
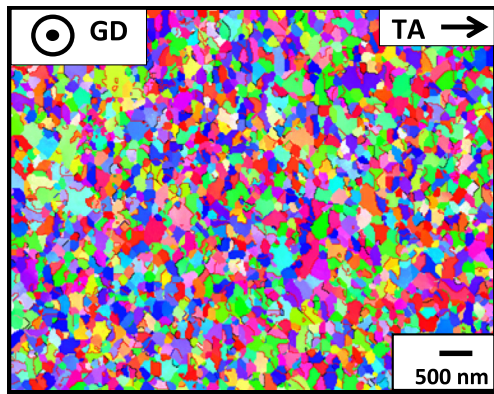
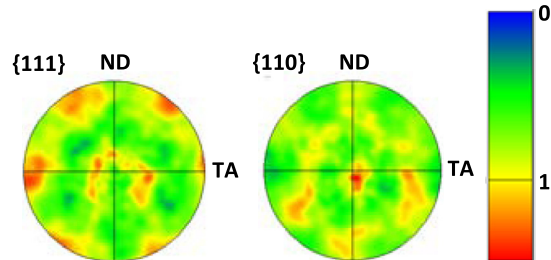
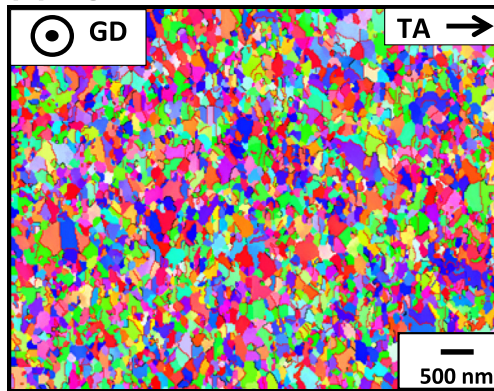
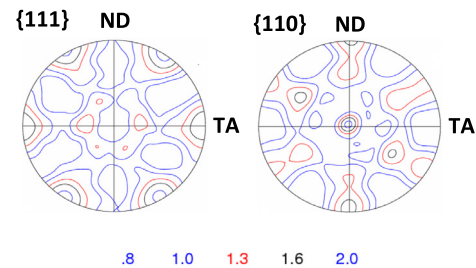
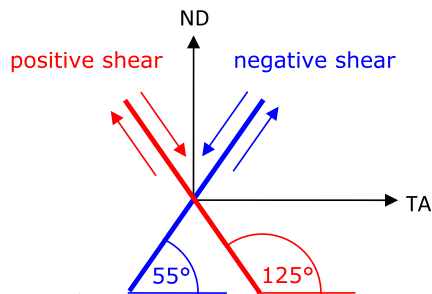
**Fig. 3.** Stress–strain curve of the sub-microcrystalline Ni specimen tested at 4 K. Inset shows the part above 2000 MPa characterized by sudden small stress drops and corresponding strain gaps. At about 2400 MPa and a plastic strain of about 1.2% sudden fracture terminated the deformation experiment as the hardening coefficient reached zero.



**Fig. 4.** (a) Sketch of the tensile specimen showing the dimensions, coordinate system (ND = normal direction, GD = growth direction, TA = tensile axis) and shear and crack traces. (b) Low magnification and (c) high magnification BSE images of the region near the crack.

Sergueeva et al., 2005). It is well known that in metallic glasses deformation and fracture do not occur along the planes of maximum shear stress (i.e. under  $45^\circ$  with respect to TA), but under  $54^\circ$  in tension and under  $43^\circ$  in compression (Zhang et al., 2003). The reason for this is the influence of the normal stress on the deformation process. Considering this it becomes obvious that the sub-microcrystalline nickel at 4 K behaves much more like an

amorphous metallic glass than like a coarse-crystalline metal polycrystal. Additionally, in Fig. 4c there are two sets of surface shear band traces on the flat surface that are inclined under  $55^\circ$ , too. It seems that both, thickness and distance of the shear bands are comparable with the grain size. Indeed, such “micro” shear bands of thickness comparable with the grain size ( $d_{\text{EBSD}} = 390 \text{ nm}$ ) separated by about 5–10  $\mu\text{m}$  have been observed by Dey et al. (2013)

**(a) initial microstructure****(b) region near crack****(c) shear systems and simulations**

**Fig. 5.** Microstructures and their related pole figures of the (a) initial microstructure and (b) near-crack region. (c) Schematic simulation diagram of the two shear systems and the corresponding simulated textures.

in cyclically deformed PED nickel. The appearance of intersecting shear bands can be explained very well on the basis of advanced simulations of localization phenomena in an aluminum alloy performed by Neale et al. (2003), using the Taylor plasticity model.

The orientation maps of the initial microstructure and that of the region near the crack (marked with *a* and *b* in Fig. 4a) with their related pole figures are given in Fig. 5a and b, respectively. Note that the orientation maps given represent just one map of many smaller ( $7.4 \times 6.8 \mu\text{m}^2$ )

EBSD acquisitions in both regions, but the pole figures are calculated from the sum of all acquisitions. The microstructure in the region near the crack is comparable to that of the initial one (compare Fig. 5a and b), however, some grain growth and very slight elongation has taken place. Earlier, more elongated grains were observed by transmission electron microscopy of thin foils normal to GD obtained through focused ion beam cutting exactly in the cracked region of a cylindrical sample deformed in tension at 4 K (Dey et al., 2010a). The reason for not observing such

pronounced elongated grains in the present EBSD image is the rupture of the most sheared region preventing EBSD very close to that. However, here like in Dey et al. (2010a) a change in texture is captured. While the initial texture is a weak fibre texture with  $\langle 110 \rangle$ ||GD, the texture in the region near the crack is considerably different and characteristic for simple shear. A similar shear texture was also reported in a flat specimen of sub-microcrystalline Ni deformed cyclically at room temperature at very high strain amplitude (Dey et al., 2010b, 2013).

The best match between the simulated and experimental texture is obtained for  $\gamma = 1.25$  and  $m = 0.1$ . The corresponding results are presented in Fig. 5b and c. The main texture components are well reproduced, however, their intensities are a little bit higher than those of the experimental ones. The reason may be the submicron grain size leading to some grain boundary sliding which is not taken into account by the VPSC model.

#### 4. Conclusions

The simple shear texture observed in the near-crack area of a flat sub-microcrystalline nickel specimen deformed in tension at 4 K clearly supports the view that localized plastic flow by shear banding is responsible for the observed discontinuous deformation mode indicated by repeated stress drops in the stress-strain curve below 2400 MPa. This stress level, probably, is a threshold stress where the shear band propagation is no longer damped by the decreasing stress level, but is accelerated by local “deformation heating” of the specimen leading to catastrophic failure. Evidently, fracture is initiated in the most sheared areas, where the inclination angle of the crack ( $55^\circ$  with respect to the tensile axis) reveals that there are similarities to shear band formation in bulk metallic glasses. It must be emphasized that the sample fractured at a plastic strain of only 0.012. Such small amount of homogeneous deformation (and moreover in tensile test conditions) usually does not change the texture. Only the proposed strain localization can lead to a sufficient amount of deformation able to change the texture in a way that corresponds to the result of the EBSD measurements in the near-crack area.

#### Acknowledgements

The authors gratefully acknowledge financial support by the Deutsche Forschungsgemeinschaft DFG, contract Sk 21/23-1. S.R. Dey and B. Beausir are grateful to the Alexander von Humboldt Foundation for their research fellowships.

#### References

Brunner, D., Diehl, J., 1992. Extension of measurements of the tensile flow-stress of high-purity alpha-iron single-crystals to very low temperatures. *Z. Metallkunde* 83, 828–834.

- Dey, S.R., Hollang, L., Reuther, K., Hübner, R., Chulist, R., Skrotzki, W., 2010a. Crystallographic characterization of catastrophic shear in submicron Ni at low temperatures. *J. Phys.: Conf. Ser.* 240, 012150.
- Dey, S.R., Hollang, L., Beausir, B., Hieckmann, E., Skrotzki, W., 2010b. Shear banding during cyclic deformation of sub-microcrystalline nickel. *Scr. Mater.* 62, 770–773.
- Dey, S.R., Hollang, L., Beausir, B., Hieckmann, E., Skrotzki, W., 2013. *Scripta Mater.*, in press. <http://dx.doi.org/10.1016/j.scriptamat.2012.12.023>.
- Engler, O., Randle, V., 2010. *Introduction to Texture Analysis – Macrotexture, Microtexture and Orientation Mapping*, second ed. CRC Press, Taylor & Francis Group, London.
- Hill, R., 1965. Continuum micro-mechanics of elastoplastic polycrystals. *J. Mech. Phys. Solids* 13, 89–101.
- Hollang, L., Hieckmann, E., Brunner, D., Holste, C., Skrotzki, W., 2006. Scaling effects in the plasticity of nickel. *Mater. Sci. Eng. A* 424, 138–153.
- Hollang, L., Reuther, K., Dey, S.R., Hieckmann, E., Skrotzki, W., 2010. Deformation mechanisms in nanocrystalline nickel at low temperatures. *J. Phys.: Conf. Ser.* 240, 012148.
- Ivanisenko, Yu., Skrotzki, W., Chulist, R., Lippmann, T., Kurmanaeva, L., 2012. Texture development in a nanocrystalline Pd–Au alloy studied by synchrotron radiation. *Scr. Mater.* 66, 131–134.
- Lebensohn, R.A., Tomé, C.N., 1993. A self-consistent anisotropic approach for the simulation of plastic-deformation and texture development of polycrystals – application to zirconium alloys. *Acta Metall.* 41, 2611–2624.
- Lüders, W., 1860. Ueber die Aeußerung der Elasticität an stahlartigen Eisenstäben und Stahlstäben, und über eine beim Biegen solcher Stäbe beobachtete Molecularbewegung. *Dinglers Polytech. J.* 155, 18–22, VIII.
- Molinari, A., Canova, G.R., Ahzi, S., 1987. A self-consistent approach of the large deformation polycrystal viscoplasticity. *Acta Metall.* 35, 2983–2994.
- Mukai, T., Nieh, T.G., Kawamura, Y., Inoue, A., Higashi, K., 2002. Effect of strain rate on compressive behaviour of a Pd<sub>40</sub>Ni<sub>40</sub>P<sub>20</sub> bulk metallic glass. *Intermetallics* 10, 1071–1077.
- Neale, K.W., Inal, K., Wu, P.D., 2003. Effects of texture gradients and strain paths on localization phenomena in polycrystals. *Int. J. Mech. Sci.* 45, 1671–1686.
- Niewczas, M., Basinski, Z.S., Basinski, S.J., Embury, J.D., 2001a. Deformation of copper single crystals to large strains at 4.2 K – I. Mechanical response and electrical resistivity. *Philos. Mag. A* 81, 1121–1142.
- Niewczas, M., Basinski, Z.S., Embury, J.D., 2001b. Deformation of copper single crystals to large strains at 4.2 K – II. Transmission electron microscopy observations of defect structure. *Philos. Mag. A* 81, 1143–1159.
- Park, L.J., Kim, H.W., Yoo, J.D., Lee, C.S., Park, K.-T., 2010. Tensile failure of 4130 steel having different ultrafine grain structures. *Mater. Sci. Eng. A* 527, 645–651.
- Rösner, H., Boucharat, N., Markmann, J., Padmanabhan, K.A., Wilde, G., 2009. In situ transmission electron microscopic observations of deformation and fracture processes in nanocrystalline palladium and Pd<sub>90</sub>Au<sub>10</sub>. *Mater. Sci. Eng. A* 525, 102–106.
- Sergueeva, A.V., Mara, N.A., Kuntz, J.D., Lavernia, E.J., Mukherjee, A.K., 2005. Shear band formation and ductility in bulk metallic glasses. *Philos. Mag. A* 85, 2671–2687.
- Tabachnikova, E.D., Podolskiy, A.V., Bengus, V.Z., Smirnov, S.N., Li, H., Liaw, P.K., Choo, H., Csach, K., Miskuf, J., 2010. Strain-rate sensitivity and failure peculiarities in compression of the nanocrystalline Ni–20 Pct Fe alloy at low temperatures. *Met. Mater. Trans.* 41A, 848–853.
- Vinogradov, A., Hashimoto, S., Patlan, V., Kitagawa, K., 2001. Atomic force microscopy study on surface morphology of ultra-fine grained materials after tensile testing. *Mater. Sci. Eng. A* 319–321, 862–866.
- Wei, Q., Jia, D., Ramesh, K.T., Ma, E., 2002. Evolution and microstructure of shear bands in nanostructured Fe. *Appl. Phys. Lett.* 81, 1240–1242.
- Yu, C.Y., Kao, P.W., Chang, C.P., 2005. Transition of tensile deformation behaviors in ultrafine-grained aluminium. *Acta Mater.* 53, 4019–4028.
- Zaiser, M., Hähner, P., 1997. A unified description of strain-rate softening instabilities. *Mater. Sci. Eng. A* 238, 399–406.
- Zhang, Z.F., Eckert, J., Schultz, L., 2003. Difference in compressive and tensile fracture mechanism of Zr<sub>59</sub>Cu<sub>20</sub>Al<sub>10</sub>Ni<sub>8</sub>Ti<sub>3</sub> bulk metallic glass. *Acta Mater.* 51, 1167–1179.